$1/f^{\alpha}$ spectra in elementary cellular automata and fractal signals

Jan Nagler[1] and Jens Christian Claussen[2,*]
[1]*Institut für Theoretische Physik, Universität Bremen, Otto-Hahn-Allee, D-28334 Bremen, Germany*
[2]*Institut für Theoretische Physik und Astrophysik, Universität Kiel, Leibnizstraße 15, D-24098 Kiel, Germany*
(Received 20 October 2004; revised manuscript received 13 April 2005; published 28 June 2005)

We systematically compute the power spectra of the one-dimensional elementary cellular automata introduced by Wolfram. On the one hand our analysis reveals that one automaton displays $1/f$ spectra though considered as trivial, and on the other hand that various automata classified as chaotic or complex display no $1/f$ spectra. We model the results generalizing the recently investigated Sierpinski signal to a class of fractal signals that are tailored to produce $1/f^{\alpha}$ spectra. From the widespread occurrence of (elementary) cellular automata patterns in chemistry, physics, and computer sciences, there are various candidates to show spectra similar to our results.

DOI: 10.1103/PhysRevE.71.067103 PACS number(s): 89.75.Da, 82.40.Np, 05.45.Df, 45.70.Qj

In 1984 Wolfram introduced the so-called elementary cellular automata (ECA), opening a field still being vividly active 20 years thereafter [1]. Wolfram's more recent popular book [2] has attracted great attention, although the opinion of the work's merits is divided among the scientific community [3]. ECA are discussed extensively in the context of computationally irreducibility of physical systems [4], e.g., it is proven that in the Turing sense [5] rule 110 (being one of the possible 256 ECA) is an universal computer [1]. Moreover, possible transformations between difference equations and (E)CA have been investigated [6]. Among the numerous physical applications we mention here only (kinetic phase transitions in) catalytic reaction-diffusion systems [7–10], deterministic surface growth [11], branching and annihilating random walks [12], and random boolean networks [13].

It is important to note that Wolfram's ECA are often studied for a particular boundary condition on a finite array which disturbs the *pure* evolution of an ECA. As a result, some automata display complex behavior, while other are simply periodic. Though there is no algorithm for classifying a given elementary automaton, Wolfram conjectured that ECA can be grouped into four classes of complexity:

Class 1: steady state; class 2: periodic or nested structures; class 3: random ("chaotic") behavior; class 4: mixture of random and periodic behavior.

The first class represents automata that are (for almost all initial conditions) trivial in the sense being static or finally evolve to the some steady state. Those rules that belong to the second class produce simple periodic or self-similar, i.e., fractal, structures. The third class includes rules exhibiting random patterns, e.g., a particular rule (number 30) is used to generate random numbers in MATHEMATICA. The fourth class is somehow a mixture of classes 2 and 3 generating the most complex structures. For more rigorous classifications we refer the reader to the literature [4,14].

Since the coining paper of Bak, Tang, and Wiesenfeld [15], there has been considerable interest in the long-time behavior of cellular automata, especially for occurrence of long range correlations, and correspondingly for power spectra exhibiting a power law decay $S(f) \sim f^{-\alpha}$ with $\alpha \approx 1.0$. Despite the abundance in nature, systems exhibiting spectra with exponents near to 1 are poorly understood. While the mechanisms generating $1/f^{\alpha}$ spectra may be substantially different from each other, some models and the observed $1/f^{\alpha}$ power laws have become a paradigm for complex dynamical systems in general [16].

Definition of ECA. An elementary cellular automaton consists of an infinite one-dimensional lattice of cells being either black (1) or white (0), and a deterministic update rule. At each discrete time step, a cell is updated, $x_n^t \to x_n^{t+1}$, according to the state of the next-neighbor sites and its own state one time step before:

$$x_n^{t+1} = f(x_{n+1}^t, x_n^t, x_{n-1}^t), \tag{1}$$

where f (the rule) is determined by eight bits being the output of the possible input bits 000, 001, …, 111. As a consequence, there are 256 (ECA) rules that are named rule 0–255. In this paper we focus on rules 90 and 150 defined by

$$x_n^{t+1} = [x_{n-1}^t + r x_n^t + x_{n+1}^t] \bmod 2, \tag{2}$$

where $r=0$ defines rule 90 and $r=1$ rule 150, respectively. As demonstrated earlier, rule 90 can be interpreted in the context of catalytic processes. A process (catalysis) is initiated (or continued) when exactly one neighbor site is active whereas the process (catalysis) is stopped when too many, i.e., two, or too less, i.e., no, neighbor sites are active [10].

A similar interpretation may be given for rule 150. Catalysis at x_n^t is stopped when no or two neighbor sites (now x_n^t included) are active and it is initiated (or continued) when one or three sites are active. Note that both rules mimic local self-limiting reaction processes [9,17].

Spectra of sum signals. It is known that ECA on finite lattices for various boundary conditions display no $1/f^{\alpha}$ spectra [1]. Rather than evaluating the rules on finite lattices we calculate the evolution on an infinite lattice. More precisely, we focus on a sum signal defined as the total *(in)activity, magnetization, etc.* of the whole system:

*Electronic address: claussen@theo-physik.uni-kiel.de

TABLE I. Rules that produce $1/f^{\alpha}$ spectra. Rules in brackets belong to one equivalence class. Rules 105 and 150 (bold) produce spectra with power law exponents about $\alpha=1.3$. All other listed rules exhibit spectra with exponents about $\alpha=1.2$. The 231 rules not listed are not capable to produce $1/f^{\alpha}$ spectra, e.g., most of the spectra display no power law decay, or exhibit *thermal* $1/f^2$ spectra (see Fig. 2).

Class	ECA rule number
1	218
2	(26, 82, 167, 181), (154, 210)
3	(18, 183), (22, 151), (60, 102, 153, 195), (90, 165), (122, 161), (126, 129), (146, 182), **105**, **150**
4	

$$X(t) = \sum_n x_n^t. \tag{3}$$

We have systematically investigated all 256 rules, for localized initial conditions (i.e., single 1, 11, 101, 111, …), as follows. The sum signal for nontrivial rules exhibits increasing mean $\langle X\rangle_t$ well fitted by a power law in time [24]. Consequently, we focus on the detrended sum signal defined by

$$Y(t) = X(t) - f(t), \tag{4}$$

where the coefficients of $f(t)=at^b$ are fitted. However, for some ECA $Y(t)$ possesses an increasing mean variance. Thus we investigate for each automaton another signal (and its spectrum)

$$Z(t) = Y(t)/\langle Y\rangle^{1/2}_{\{t-l+1,t+l\}}, \tag{5}$$

where $2l$ is the width of a sliding window that normalizes the fluctuations of the detrended signal $Y(t)$ according to the method of detrended fluctuation analysis (DFA) applied for nonequilibrium processes [18]. We have calculated the corresponding power spectra $|X(\omega)|^2$, $|Y(\omega)|^2$, and $|Z(\omega)|^2$ for all 256 ECA. It turns out that that 25 of the 256 rules exhibit $1/f^{\alpha}$ spectra whereas 231 do not (see Table I). Twenty-three of those automata that exhibit $1/f^{\alpha}$ spectra display Sierpinski patterns, i.e., well studied self-similar structures [10]. Their spectra are extensively investigated in Ref. [10] exhibiting $1/f^{\alpha}$ spectra with exponents 1.15 ± 0.05.

The two other rules, i.e., 105 and 150, show a different behavior. Here we focus on rule 150 [25]. The first 128 time steps of the evolution for a single 1 as the initial condition is depicted in Fig. 1 (upper inset).

It is a Sierpinski-like self-similar structure. However, the fractal dimension differs from the Sierpinski gasket ($d=1.58$) being the golden mean $d=(1+\sqrt{5})/2\approx1.69$. Figure 1 shows also the corresponding signals $X(t)$ and $Z(t)$. The spectrum $Y(\omega)$ is displayed in Fig. 2. For ω not too small, the averaged spectrum exhibits a straight line in the log-log plot verifying a power law behavior. Depending on the average process and fit range we obtain a fit exponent of about $\alpha=1.27\pm0.05$. Due to dominating randomness, members of classes 3 and 4 typically produce thermal $1/f^2$ spectra (see Fig. 2).

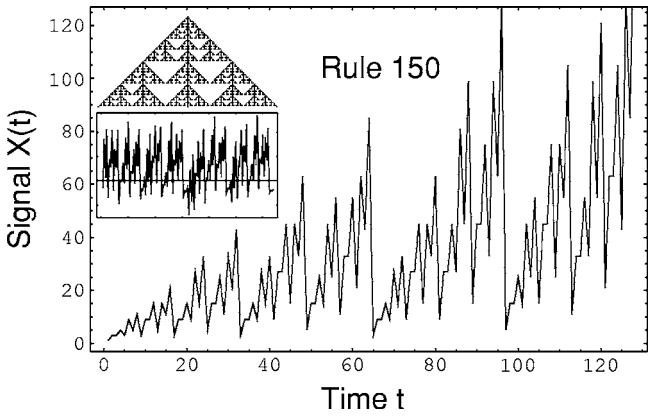

FIG. 1. The first 128 time steps of the time signal $X(t)$ generated by rule 150. Upper inset: self-similar structure generated by rule 150 for the first 64 time steps. Lower inset: normalized signal $Z(t)$; the straight line indicates $Z=0$.

Fractal signals produce $1/f^{\alpha}$ *spectra*. All ECA that are capable to produce a self-similar structure exhibit $1/f^{\alpha}$ spectra. Hence one may naively expect that every (self-similar) fractal structure produces $1/f^{\alpha}$ spectra. However, it is important to know that this is not the case. There are many fractals like the Koch snow flake, Cantor dust, etc., exhibiting no $1/f^{\alpha}$ spectra because their respective sum signals simply grow exponentially [19].

Rather than a geometric approach we focus on fractal *signals* itself. Thus we now generalize the recently investigated Sierpinski signal [10]. As we will see, the generalized signal is capable to model $1/f^{\alpha}$ spectra producing spectra with continuously tunable power law exponents. More precisely, we consider the signal

$$X_{\delta}(t) = 2^{\delta\Sigma_j \sigma_j\{t\}}, \tag{6}$$

where σ_j is the jth bit of the binary decomposition of the discrete time $t=0, 1, 2, \ldots$. For $\delta=1$ we have shown recently

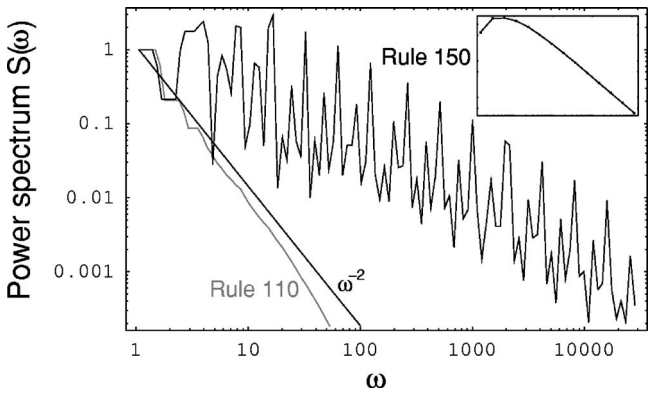

FIG. 2. Rule 150 and rule 110: Averaged power spectrum of $Y(t)$ up to $T/8$ for $T=2^{18}$ using (incommensurable) 1.1^k bins, i.e., the kth interval is defined by $[\lceil 1.1^k\rceil,\lceil 1.1^{k+1}\rceil]$ where the brackets $\lceil\ \rceil$ denote upwards rounded integer values (ceiling function). The inset shows the rule 150 spectrum, averaged using 2^k bins, i.e., the kth interval is defined by $[2^k, 2^{k+1}-1]$. Both averages correspond to a constant $\delta\omega/\omega$ ratio. The graphs are well fitted by a power law with exponent $\alpha=1.27$. The thermal $1/f^2$ decay of rule 110 (gray) as a typical member of class 4 is shown for comparison.

both numerically and analytically that the signal exhibits $1/f^{\alpha}$ spectra with α close to unity. The special ansatz, Eq. (6), represents a straightforward generalization of the closed form for the sum signal of the Sierpinski pattern produced by rule 90 [10]. In the next paragraph we show that for deviations from $\delta=1$ the signal can produce $1/f^{\alpha}$ spectra within a wide range of exponents α.

In analogy to the calculation in Ref. [10], we calculate the periodogram $X(\omega)$ of the time signal (6) analytically:

$$\begin{aligned} X(\omega) &= \sum_{t=0}^{2^N-1} e^{i\omega t} X_\delta(t) \\ &= \sum_{\{\sigma_0,\ldots,\sigma_{N-1}\}} \exp\left(i\omega \sum_j \sigma_j 2^j\right) X_\delta\left(\sum_j \sigma_j 2^j\right) \\ &= \sum_{\{\sigma_0,\ldots,\sigma_{N-1}\}} \prod_{j=0}^{N-1} \exp[\sigma_j(i\omega 2^j + \delta \ln 2)] \\ &= \prod_{j=0}^{N-1} \sum_{\{\sigma_j\}} \exp[\sigma_j(i\omega 2^j + \delta \ln 2)] \\ &= \prod_{j=0}^{N-1} [1 + \exp(i\omega 2^j + \delta \ln 2)]. \end{aligned} \tag{7}$$

The absolute value of $X(\omega)$ simplifies to a trigonometric product which the logarithm converts into a sum:

$$\ln|X(\omega)|^2 = \sum_{j=0}^{N-1} \ln[1 + 2^{2\delta} + 2^{1+\delta}\cos(\omega 2^j)]. \tag{8}$$

We roughly estimate the sum in Eq. (8) replacing the sum by an integral, and substituting $y=\omega 2^j$,

$$\ln|X(\omega)|^2 \approx \int_0^{N-1} \ln[1 + 2^{2\delta} + 2^{1+\delta}\cos(\omega 2^j)]dj \tag{9}$$

$$= \int_{\omega}^{\omega 2^{N-1}} \frac{\ln[1 + 2^{2\delta} + 2^{1+\delta}\cos y]}{y \ln 2} dy. \tag{10}$$

As $\ln(a+bx) \approx \ln(a) + (b/a)x$ for $|x| \ll 1$, we obtain

$$\ln|X(\omega)|^2 \approx \frac{\ln(1+2^{2\delta})}{\ln 2} \int_{\omega}^{\omega 2^{N-1}} \frac{dy}{y} + \frac{2^{1+\delta}}{(1+2^{2\delta})\ln 2} \int_{\omega}^{\omega 2^{N-1}} \frac{\cos(y)}{y} dy. \tag{11}$$

The integral over the integral cosine is nearly independent of the upper boundary for high values of the boundary. Thus we can substitute the upper boundary $\omega 2^{N-1}$ by some N-dependent constant, say $c_N \gg 1$. Finally, replacing the cosine by one yields immediately a rough approximation of the power spectrum:

$$|X(\omega)|^2 \approx c'_N \omega^{-(2^{1+\delta})/(1+2^{2\delta})\ln 2}. \tag{12}$$

For a given power law exponent $0 < \alpha \leqslant 1/\ln 2 \approx 1.44$, we obtain δ from Eq. (12) as

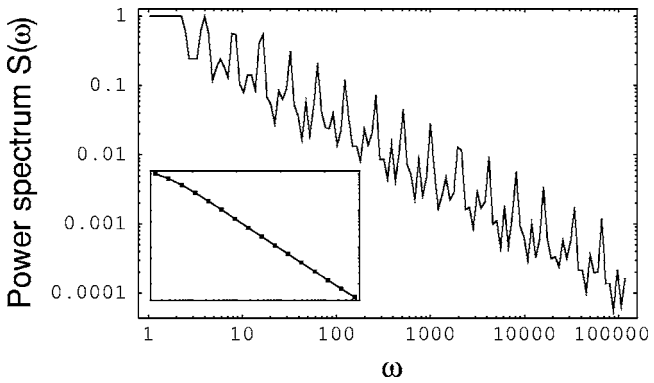

FIG. 3. Averaged power spectrum of the detrended signal (6) for $\delta=1.311\,84$ up to $T/8$, $T=2^{20}$ using (incommensurable) 1.1^k bins. The inset shows the spectrum, averaged using 2^k bins. Both correspond to a constant $\delta\omega/\omega$ ratio. Fit exponents of about $\alpha=0.93$. The corresponding spectrum for the variance detrended signal exhibits power spectra around $\alpha=1.0$. The theoretical exponent is $\alpha=1.0$.

$$\delta = \frac{\ln\left(\frac{1+\sqrt{1-\alpha^2(\ln 2)^2}}{\alpha \ln 2}\right)}{\ln 2}. \tag{13}$$

To generate signals with goal exponents, e.g., $\alpha_1=0.8$, $\alpha_2=1.0$, $\alpha_3=1.2$, one can use the corresponding value of δ according to Eq. (13). Figure 3 shows the spectrum of the detrended signal (6) for $\delta_2=1.311\,84$ (corresponding to $\alpha_2=1.0$). For $\delta_1=1.724\,25$ and $\delta_3=0.902\,749$ the individual spectra exhibit similar graphs (not shown). Depending on the averaging the power law fits giving $\alpha_1=0.8\pm0.1$, $\alpha_2=0.95\pm0.05$, and $\alpha_3=1.2\pm0.05$, are in good agreement with the theoretical results.

Two-dimensional automaton. While one-dimensional experimental setups as in Ref. [17] seem to be quite artificial for (self-limiting) catalytic processes, two-dimensional dynamics is more generic [23]. Consider the Sierpinski dynamics on a (i,j) plane:

$$x_{i,j}^{t+1} = [x_{i+1,j}^t + x_{i-1,j}^t + x_{i,j+1}^t + x_{i,j-1}^t] \bmod 2. \tag{14}$$

For a single 1 as initial condition on a plane the sum signal $X_{2D}(t)=\Sigma_{i,j}\, x_{i,j}^t$ generates the sequence

$$X_{2D}(t) = 1,4,4,16,4,16,16,64,\ldots\,. \tag{15}$$

More precisely, the recurrence relation generating Eq. (15) is given by $u_n \to u_{n+1}=(u_n, 4u_n)$ for $u_0=(1)$.

First, if the factor 4 is replaced by 2, the relation becomes equivalent to the one-dimensional-Sierpinski signal $X_{1D}(t)$ in Ref. [10]. Second, we obtain $X_{2D}(t)=X_{1D}(t)^2$ and therefore $X_{2D}(t)=X_{\delta=2}(t)$. Thus the generalized Sierpinski pattern in two dimensions exhibits $1/f^{\alpha}$ spectra with exponents around the value according to Eq. (12) for $\delta=2$, that is, $\alpha=0.679$. We numerically verified the value obtaining exponents around $\alpha=0.7$ as expected.

Multifractality. The spectral analysis applied so far assumes implicitly monofractal signals. Multifractal spectra [20] for signals $X_\delta(t)$, being binomial multifractal series, can be calculated analytically [21,22]:

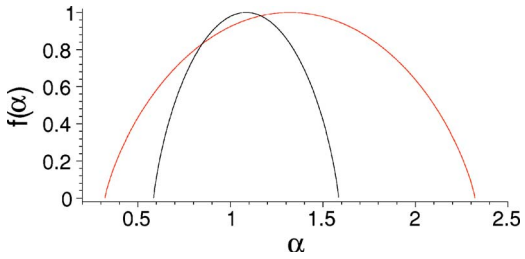

FIG. 4. (Color online) Multifractal spectra for signals $X_{1D}(t)$ (black) and X_{2D} [red (gray)]. Maxima positions: $\alpha_{1D}=1.08$, $\alpha_{X_{2D}}=1.32$.

$$f(\alpha) = d(\xi(\alpha)), \text{ where} \tag{16}$$

$$d(\xi) = -\frac{\xi \ln(\xi) + (1-\xi)\ln(1-\xi)}{\ln 2}, \text{ and} \tag{17}$$

$$\xi(\alpha) = -\frac{\alpha \ln(2) + \ln(1-a)}{\ln(a) - \ln(1-a)}, \tag{18}$$

for $a=2^{\delta}/(1+2^{\delta})$. Figure 4 displays the multifractal spectra for the signals $X_{1D}(t)$, and $X_{2D}(t)$, corresponding to the parameters $a_{1D}=2/3$, $a_{2D}=4/5$ in Ref. [21]. The spectra have the typical inverse U-shaped form.

Conclusions. Elementary cellular automata represent a paradigm for emergence of complex spatiotemporal dynamics of widespread relevance. We systematically investigated all 256 elementary cellular automata. As expected, among those as (nested) periodic or chaotic classified rules (classes 2 and 3) there are various rules that display $1/f^{\alpha}$ spectra (see Table I). Unexpectedly, on the one hand all rules classified as complex display *no* $1/f^{\alpha}$ spectra, while on the other hand, the *trivial* rule 218 does (being a member of class 1). It is important to note that the numerically calculated spectra are robust against noise, that is, the fit exponents change only slightly for other initial conditions than a single seed.

Moreover, we generalized the approach of a sum signal introduced in Ref. [10] for two reasons. First, the investigated fractal signals (6) serve as a fit model for the total (in)activity of one-dimensional ECA. Second, (Sierpinski) dynamics in two dimensions is more generic [2,23]. Therefore we derived analytically the spectra of the two-dimensional Sierpinski automaton. The tailored signals represent analytically tractable (nontrivial) $1/f^{\alpha}$ generators with continuously tunable power law decay exponent. Consequently, our analysis may shed light on the arcane mechanisms of $1/f^{\alpha}$ spectra.

From our results, we expect that in experimental systems showing spatiotemporal pattern formation similar to the ECA patterns, the power spectra of the total (in)activity will exhibit power law behavior within a certain range.

[1] S. Wolfram, Physica D **10**, 1-35 (1984); Nature (London) **311**, 419 (1984); Rev. Mod. Phys. **55**, 601 (1983).
[2] S. Wolfram, *A New Kind of Science* (Wolfram Media, Champaign, Illinois 2002); http://www.wolframscience.com/nksonline/toc.html
[3] J. Giles, Nature (London) **417**, 216 (2002).
[4] Navot Israeli and Nigel Goldenfeld, Phys. Rev. Lett. **92**, 074105 (2004).
[5] *The Universal Turing Machine, A Half-Century Survey*, edited by R. Herken (Springer-Verlag, Wien, 1995).
[6] A. Nobe, J. Satsuma, and T. Tokihiro, J. Phys. A **34**, L371 (2001).
[7] Robert M. Ziff, Erdagon Gulari, and Yoav Barshad, Phys. Rev. Lett. **56**, 2553 (1986).
[8] Y. Hayase, J. Phys. Soc. Jpn. **66**, 2584 (1987); Y. Hayase and T. Ohta, Phys. Rev. Lett. **81**, 1726 (1998); Y. Hayase and T. Ohta, Phys. Rev. E **62**, 5998 (2000).
[9] A. W. M. Dress, M. Gerhardt, N. I. Jaeger, P. J. Plath, H. Schuster, in *Temporal Order*, edited by L. Rensing and I. Jaeger (Springer, Berlin, 1984).
[10] Jens Christian Claussen, Jan Nagler, and Heinz Georg Schuster, Phys. Rev. E **70**, 032101 (2004).
[11] J. Krug and H. Spohn, Phys. Rev. A **38**, 4271 (1988).
[12] John Cardy and Uwe C. Täuber, Phys. Rev. Lett. **77**, 4780 (1996).
[13] Mihaela T. Matache, and Jack Heidel, Phys. Rev. E **69**, 056214, (2004).
[14] V. C. Barbosa, F. M. N. Miranda, and M. C. M. Agostini, e-print nlin.CG/0408014.
[15] P. Bak, C. Tang, and K. Wiesenfeld, Phys. Rev. Lett. **59**, 381 (1987); Phys. Rev. A **38**, 364 (1988).
[16] H. J. Jensen, *Self-Organized Criticality* (Cambridge University Press, Cambridge, England, 1998).
[17] R. D. Otterstedt, N. I. Jaeger, P. J. Plath, and J. L. Hudson, Phys. Rev. E **58**, 6810 (1998).
[18] K. Hu, P. C. Ivanov, Z. Chen, P. Carpena, and H. E. Stanley, Phys. Rev. E **64**, 011114 (2001).
[19] Benoit B. Mandelbrot, *Multifractals and* $1/f$ *Noise* (Springer, New York, 1999); *Fractals and Chaos* (Springer, New York, 2004).
[20] T. C. Halsey *et al.*, Phys. Rev. A **33**, 1141 (1986).
[21] J. W. Kantelhardt, S. A. Zschiegner, A. Bunde, S. Havlin, E. Koscielny-Bunde, and H. E. Stanley, Physica A **316**, 87 (2002); S. Zschiegner, Diploma thesis, Justus Liebig Universität, Göttingen, 2002.
[22] J. Feder, *Fractals* (Plenum Press, New York, 1988).
[23] Y. Gefen, A. Aharony, B. B. Mandelbrot, and S. Kirkpatrick, Phys. Rev. Lett. **47**, 1771 (1981).
[24] In Ref. [10] we have shown this both numerically and analytically for rule 90. For other rules it is also easy to derive analytically.
[25] Rule 105 is simply the inverse of rule 150, i.e., $f_{105}(a,b,c) = 1 - f_{150}(a,b,c)$.